NT@UW-98-33

Tensor Polarized γ-Deuteron Compton Scattering in Effective Field Theory

Jiunn-Wei Chen*
Department of Physics, University of Washington, Seattle, WA 98195-1560, USA

Abstract

The differential cross section for γ-deuteron Compton scattering from a tensor polarized deuteron is computed in an effective field theory. The first non-vanishing contributions to this differential cross section are the interference terms between the leading electric coupling diagrams and the subleading single potential pion exchange diagrams or the subleading magnetic moment coupling diagrams. At 90° photon scattering angle, only the pion term contributes at this order to the tensor polarized differential cross section. This provides a clean way to study the photon pion dynamics in the two nucleon sector. The effect is measurable for photon energies between 40 and 80 MeV provided the uncertainty in the measured cross sections are $\lesssim 7\%$.

*jwchen@phys.washington.edu

I. INTRODUCTION

γ-deuteron Compton scattering probes the structure of the deuteron and provides necessary information that may allow the extraction of neutron properties, such as neutron electric and magnetic polarizabilities. The differential cross section of unpolarized γ-deuteron Compton scattering has been measured at incident photon energies of 49 MeV and 69 MeV with 10% uncertainty [1]. Theoretical calculations based on potential models and taking the nucleon polarizabilities as inputs find reasonably good agreement with data [2–4] but are not sufficient to give tight constraints on the nucleon polarizabilities.

In comparison to potential model calculations, a model independent, parameter free and analytic computation of unpolarized γ-deuteron Compton scattering based on a recently developed nucleon-nucleon effective field theory [5–27] was presented in [28]. Contributions up to next-to-leading order (NLO) in the effective field theory expansion including diagrams contributing to the nucleon polarizabilities give excellent agreement with the data at 49 MeV and reasonable agreement with the data at 69 MeV. At this order (NLO), the agreement with the data is comparable to the agreement between the data and potential model calculations [2,3], while inclusion of the next-next-to-leading order (NNLO) contributions should reduce the theoretical uncertainty from 10% to a few percent level.

In addition to γ-deuteron Compton scattering, the effective field theory technique also successfully describes the NN scattering phase shifts up to center-of-mass momenta of $\mathbf{p} \sim 300$ MeV per nucleon [23] in all partial waves. The electromagnetic moments, form factors [24] and polarizability [29] of the deuteron as well as parity violation in the two-nucleon sector [30] also have been explored with this new effective field theory. The results all agree with data (where available) within the uncertainty from neglecting higher order effects.

In the case of polarized γ-deuteron Compton scattering, no experiments have been performed so far. Planned experiments at TUNL to examine the Gerasimov-Drell-Hearn (GDH) sum rule using a circularly polarized photon beam will be the first attempt to study vector polarized γ-deuteron Compton scattering. Experiments using tensor polarized targets are also technically feasible. Existing technologies like spin-exchange optical pumping [31], which will be applied in the BLAST polarized ^{1}H and ^{2}H laser driven sources, and free electron lasers can provide high quality polarized deuteron targets and photon beams. The question is, what kind of physics can be measured in such an experiment? Is it interesting enough to motivate the experiments?

Theoretically, four vector form factors (corresponding to the $\Delta J = 1$ interaction of the deuteron field) and six tensor form factors (corresponding to $\Delta J = 2$) are identified in [32,33] with the lower multipole contributions calculated using dispersion relations and potential models. In this paper, we perform an analytic calculation of the differential cross section of the tensor polarized γ-deuteron Compton scattering cross section to first non-vanishing order in the effective field theory expansion. At this order, the contributions to the cross section from the $\Delta J = 2$ amplitude are the interference terms between the leading electric coupling diagrams and the subleading single potential pion exchange diagrams or the subleading magnetic moment coupling diagrams. Thus the pion effects are of leading order. We can further isolate the pion contribution by setting the photon scattering angle to be 90°. At this angle, only the pion term contributes at this order to the tensor polarized differential cross section. This provides a clean way to study the photon pion dynamics in

the two nucleon sector. The experimental precision required to measure these effects will also be discussed in the following sections.

II. TENSOR POLARIZED γ-DEUTERON COMPTON SCATTERING

The process we will focus on is the low energy (below pion production threshold) tensor polarized Compton scattering

$$\gamma(\omega,\mathbf{k})\overset{\leftrightarrow}{d}\rightarrow\gamma(\omega^{'},\mathbf{k}^{'})d \quad , \tag{2.1}$$

where the incident photon of four momentum $(\omega,\mathbf{k})$ in the deuteron rest frame (lab frame) scatters off the polarized deuteron target to an outgoing photon of four momentum $(\omega^{'},\mathbf{k}^{'})$. The polarization of photons and final state deuteron are not detected. For convenience, we will work in the lab frame and choose the $\mathbf{k}$ direction to be the (0,0,1) direction. The scattering amplitude can be written in terms of scalar, vector and tensor form factors S, V, and T corresponding to the $\Delta J = 0, 1, 2$ interactions of the deuteron field,

$$\mathcal{M} = i\frac{e^2}{M_N}\left\{S\varepsilon_d{\cdot}\varepsilon_d^{'*} + \varepsilon_{ijk}V_i\varepsilon_{d_j}\varepsilon_{d_k}^{'*} + T_{ij}\left(\varepsilon_{d_i}\varepsilon_{d_j}^{'*} + \varepsilon_{d_j}\varepsilon_{d_i}^{'*} - \tfrac{2}{3}\delta_{ij}\varepsilon_d{\cdot}\varepsilon_d^{'*}\right)\right\} \quad , \tag{2.2}$$

where ε_d and $\varepsilon_d^{'}$ are the polarization vectors of the initial and final state deuterons. Using the power counting described in [28], the scalar form factor S contributes to the amplitude starting at leading order (LO) in the effective field theory expansion, while the tensor form factor T and the vector form factor V contribute starting at next-to-leading order (NLO) and next-next-to-leading order (NNLO) respectively. Squaring the amplitude to form the cross section, the LO contribution to the cross section only comes from the $|S|^2$ term which is independent of the deuteron target polarization, while the target polarization dependent S and T interference term contributes at NLO. Note that the vector form factor V does not contribute to the cross section through the S and V interference term since the final state deuteron polarization is not detected.

It is useful to define the tensor polarized differential cross section $d\sigma_2$ as a tensor combination of polarized differential cross sections to eliminate the LO polarization independent effect and make the S and T contribution become leading. $d\sigma_2$ is defined by

$$\frac{d\sigma_2}{d\Omega} \equiv \frac{1}{4}\left[2\frac{d\sigma}{d\Omega}(J_z=0) - \frac{d\sigma}{d\Omega}(J_z=+1) - \frac{d\sigma}{d\Omega}(J_z=-1) \quad \right] \quad , \tag{2.3}$$

where J_z indicates the polarization of the deuteron target. We have

$$\begin{aligned} J_z = 0 \quad , \quad \varepsilon_d = (0,0,1) \quad ; \\ J_z = \pm 1 \quad , \quad \varepsilon_d = \frac{1}{\sqrt{2}}(1,\pm i,0) \quad . \end{aligned} \tag{2.4}$$

To predict $d\sigma_2$, we need expressions for S and T. The calculation of the scalar form factor S was carried out up to NLO in [28]. Two distinct structures contributing to S can be parameterized by electric and magnetic form factors F_0 and G_0 as

$$S = F_0\varepsilon\cdot\varepsilon^{'*} + G_0\ (\widehat{\mathbf{k}}\times\varepsilon\ )\cdot(\widehat{\mathbf{k}}'\times\varepsilon^{'*}) \quad , \tag{2.5}$$

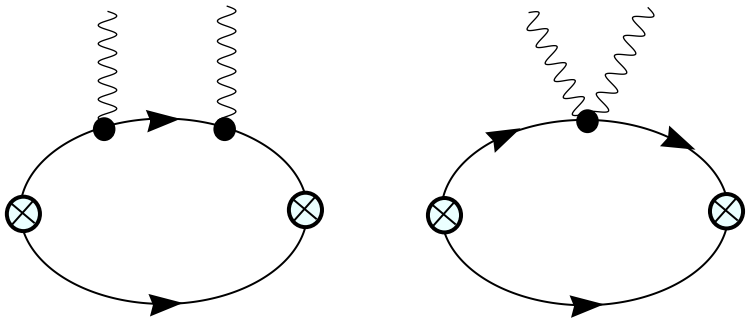

FIG. 1. *Leading order contributions to the scalar form factor of γ-deuteron Compton scattering. The crossed circles denote operators that create or annihilate two nucleons with the quantum numbers of the deuteron. The dark solid circles correspond to the photon coupling via the nucleon kinetic energy operator (minimal coupling). The solid lines are nucleons. The photon crossed graphs are not shown.*

where ε and $\varepsilon^{'}$ are the polarization vectors of the initial and final state photons, $\widehat{\mathbf{k}}$ and $\widehat{\mathbf{k}}'$ are unit vectors in the direction of $\mathbf{k}$ and $\mathbf{k}'$. At LO (denoted by a superscript on the form factors), F_0 receives contributions from the electric coupling of the $N^\dagger \mathbf{D}^2 N$ operator (minimal coupling), as shown in Fig. 1, to be

$$F_0^{LO} = -\left[\frac{\sqrt{2}\gamma}{|\omega|\sqrt{1-\cos\theta}}\tan^{-1}\left(\frac{|\omega|\sqrt{1-\cos\theta}}{2\sqrt{2}\gamma}\right) + \frac{2\gamma^4}{3M_N^2\omega^2} - \frac{2\gamma(\gamma^2 - M_N\omega - i\epsilon)^{3/2}}{3M_N^2\omega^2}\right] + [\omega \to -\omega] \quad , \tag{2.6}$$

where $\cos\theta = \widehat{\mathbf{k}}\cdot\widehat{\mathbf{k}}'$ is the cosine of the angle between the incident and outgoing photons and $\gamma = \sqrt{M_N B}$ is the deuteron binding momentum. In eq. (2.6) terms suppressed by additional factors of $\mathbf{k}^2/(m_N\omega)$ (i.e., recoil effects) are neglected since they only contribute to NNLO differential cross sections. At LO, the magnetic contribution vanishes,

$$G_0^{LO} = 0 \quad . \tag{2.7}$$

We do not show the NLO results for F_0 and G_0 here since we only calculate $d\sigma_2$ to its first non-vanishing order.

The tensor form factor T has more distinct structures. However, up to NLO, after neglecting pion contributions suppressed by factors of $\mathbf{k^2}/m_\pi^2$, T can be parameterized by electric and magnetic form factors F_2 and G_2 as

$$T_{ij} = F_2\varepsilon_i\varepsilon_j^{'*} + G_2\ (\widehat{\mathbf{k}}\times\varepsilon\ )_i(\widehat{\mathbf{k}}^{'}\times\varepsilon^{'*})_j \quad . \tag{2.8}$$

F_2 and G_2 are related to the form factors $P2(E1,E1)$ and $P2(M1,M1)$ defined in [32,33] by a normalization factor. At LO, F_2 and G_2 vanish,

$$F_2^{LO} = 0 \quad , \quad G_2^{LO} = 0 \quad . \tag{2.9}$$

At NLO F_2 receives contributions from the electric coupling of the one potential pion exchange diagrams shown in Fig. 2 and gives a renormalization scale μ independent contribution

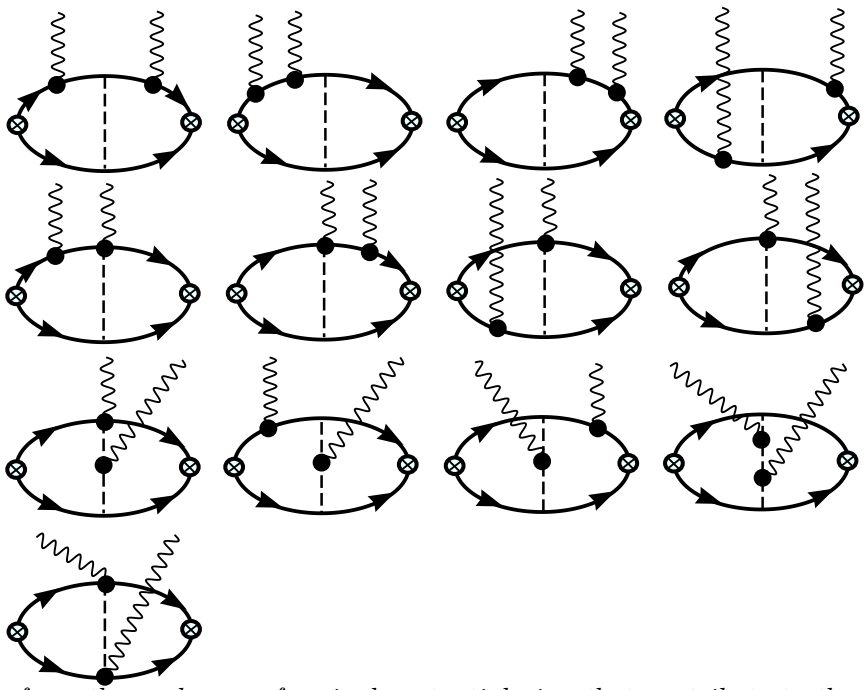

FIG. 2. *Graphs from the exchange of a single potential pion that contribute to the tensor form factor of γ-deuteron Compton scattering at NLO. The crossed circles denote operators that create or annihilate two nucleons with the quantum numbers of the deuteron. The solid circles correspond to the photon coupling via the nucleon or meson kinetic energy operator (minimal coupling) or from the gauged axial coupling to the meson field. Dashed lines are mesons and solid lines are nucleons. Photon crossed graphs are not shown.*

$$
\begin{aligned}
F_2^{NLO} = \frac{g_A^2\gamma}{240\pi f^2 M_N\omega^2}\Bigg\{ & \left[m_\pi^2(17m_\pi^2-28\gamma^2)-24M_N^2\omega^2\right]\log\left[\frac{m_\pi+2\gamma}{\mu}\right] \\
& - m_\pi^2(m_\pi^2+4\gamma^2-4M_N\omega)\log\left[\frac{m_\pi+2\sqrt{\gamma^2-M_N\omega-i\epsilon}}{\mu}\right] \\
& - 8\left[m_\pi^2(2m_\pi^2-4\gamma^2+M_N\omega)-3M_N^2\omega^2\right]\log\left[\frac{m_\pi+\gamma+\sqrt{\gamma^2-M_N\omega-i\epsilon}}{\mu}\right] \\
& + \frac{32M_N\omega\left[2m_\pi\gamma^2-M_N\omega(m_\pi-\gamma)\right]}{m_\pi+\gamma+\sqrt{\gamma^2-M_N\omega-i\epsilon}} \\
& + \frac{4M_N^2\omega^2(5m_\pi^2-12\gamma^2)}{(m_\pi+2\gamma)^2} \\
& - 2\left[m_\pi^3+4\left(2m_\pi^2-M_N\omega\right)(m_\pi-\gamma)\right]\left(\gamma-\sqrt{\gamma^2-M_N\omega-i\epsilon}\right)\Bigg\} \\
& + \{\omega\to-\omega\} \quad , \qquad (2.10)
\end{aligned}
$$

where $f = 132$ MeV is the pion decay constant. In the computation of the pion diagrams, the pion propagators with photon momentum dependence have the form

$$
\frac{1}{-(p_0-\omega)^2+(\mathbf{p}-\mathbf{k})^2+m_\pi^2} \approx \frac{1}{\mathbf{p}^2-2\mathbf{p}\cdot\mathbf{k}+m_\pi^2} \quad , \qquad (2.11)
$$

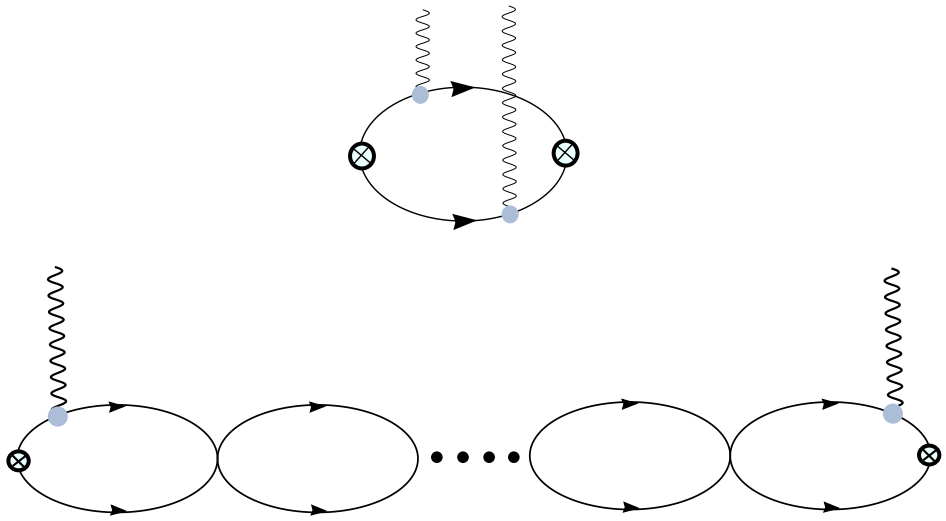

FIG. 3. *Graphs from insertions of the nucleon magnetic moment interaction that contribute to the tensor form factor of γ-deuteron Compton scattering at NLO. The crossed circles denote operators that create or annihilate two nucleons with the quantum numbers of the deuteron. The light solid circles denote the nucleon magnetic moment operator. The solid lines are nucleons. The bubble chain arises from insertions of the four nucleon operator with coefficient $C_0^{(^1S_0)}$ or $C_0^{(^3S_1)}$.*

where $(p_0, \mathbf{p})$ is the loop momentum. p_0 is of higher order in the power counting compared with the other scales in the propagators and can be neglected. We keep the first term in the $\mathbf{k}$ expansion of the pion propagators to get the result of eq. (2.10). The error of this approximation is of order $\mathbf{k}^2/m_\pi^2$ of eq. (2.10) and of even higher order in powers of $\mathbf{k}^2/m_\pi^2$ at $\theta = 0$ and $\theta = \pi$. Because the error is formally of NLO in power counting, strictly speaking we have not presented the complete calculation at NLO. However, numerically the terms omitted are NNLO.

The magnetic moment coupling diagrams shown in Fig. 3 contribute to G_2 at NLO as

$$\begin{aligned} G_2^{NLO} = & -\frac{2(\kappa^{(0)^2} - \kappa^{(1)^2})\gamma(\gamma - \sqrt{\gamma^2 - M_N\omega - i\epsilon})}{M_N^2} \\ & + \frac{\kappa^{(1)^2}\gamma(\gamma - \sqrt{\gamma^2 - M_N\omega - i\epsilon})^2 \mathcal{A}_{-1}^{(^1S_0)}(\omega - B)}{2\pi M_N} \\ & - \frac{\kappa^{(0)^2}\gamma(\gamma - \sqrt{\gamma^2 - M_N\omega - i\epsilon})^2 \mathcal{A}_{-1}^{(^3S_1)}(\omega - B)}{2\pi M_N} \\ & + (\omega \to -\omega) \quad , \end{aligned} \tag{2.12}$$

where $\kappa^{(0)} = (\kappa_p + \kappa_n)/2$ and $\kappa^{(1)} = (\kappa_p - \kappa_n)/2$ are isoscalar and isovector nucleon magnetic moments in nuclear magnetons, with $\kappa_p = 2.79285$ and $\kappa_n = -1.91304$. The leading order nucleon nucleon scattering amplitudes contribute to the magnetic moment diagrams through the C_0 bubble chains and has the expression [23,24]

$$\mathcal{A}_{-1}^{(^1S_0),(^3S_1)}(\omega - B) = \frac{-C_0^{(^1S_0),(^3S_1)}}{1 + C_0^{(^1S_0),(^3S_1)}\frac{M_N}{4\pi}(\mu - \sqrt{-M_N(\omega - B) - i\varepsilon}\ )} \quad . \tag{2.13}$$

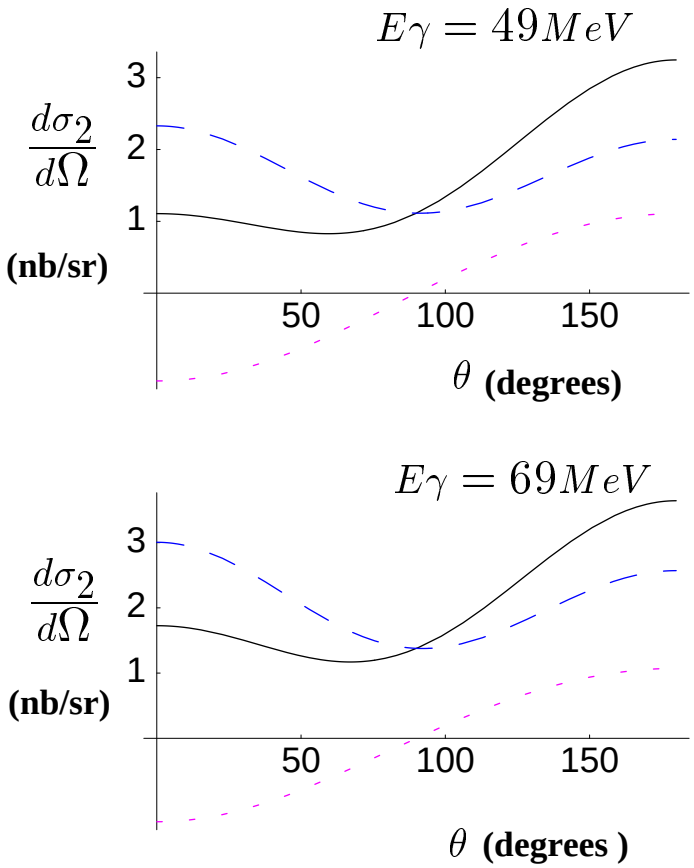

FIG. 4. *The differential cross section for tensor polarized γ-deuteron Compton scattering to first non-vanishing order at incident photon energies of $E_\gamma = 49$ MeV and 69 MeV. The dashed curves correspond to the pion interference term contributions. The dotted curves correspond to the magnetic moment interference term contributions. The solid curves correspond to the sum of the pion and magnetic moment interference terms.*

The renormalization scale μ dependence in the denominator is canceled by the μ dependence of $C_0^{(^1S_0)}$ and $C_0^{(^3S_1)}$, as required. Values of $C_0^{(^1S_0)}$ and $C_0^{(^3S_1)}$ have been determined from nucleon nucleon scattering in the $^1S_0$ and $^3S_1$ channels [23,24] to be $C_0^{(^1S_0)} = -3.34$ fm^2 and $C_0^{(^3S_1)} = -5.51$ fm^2 at $\mu = m_\pi$.

Having obtained the leading non-vanishing contributions for S and T, we now give the leading non-vanishing expressions for $d\sigma_2$. At LO, $d\sigma_2$ vanishes,

$$\frac{d\sigma_2^{LO}}{d\Omega} = 0 \quad . \tag{2.14}$$

While at NLO,

$$\frac{d\sigma_2^{NLO}}{d\Omega} = \frac{\alpha^2}{2M_N^2}\left[Re[F_0^{LO}F_2^{NLO^*}](1+\cos^2\theta) + 2Re[F_0^{LO}G_2^{NLO^*}]\cos\theta\right] \quad . \tag{2.15}$$

There are two terms in $d\sigma_2^{NLO}$. The first term comes from the interference between the LO electric coupling diagrams and the NLO one potential pion exchange diagrams. The

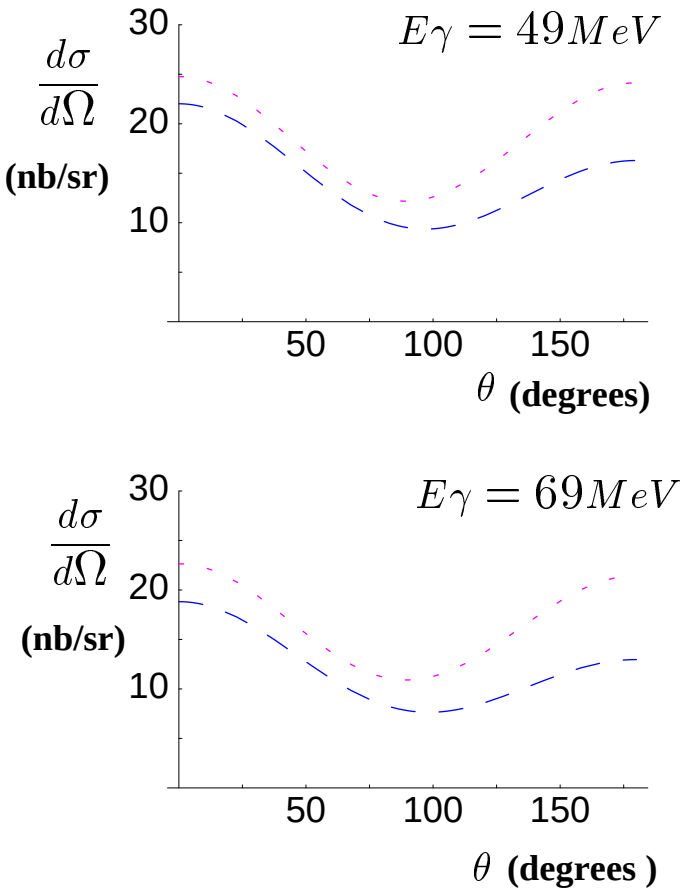

FIG. 5. *The differential cross section for polarized γ-deuteron Compton scattering at incident photon energies of $E_\gamma = 49$ MeV and 69 MeV. The dotted curves correspond to the NLO deuteron $J_z = 0$ result. The dashed curves correspond to the NLO deuteron $J_z = 1$ result.*

second term comes from the interference between the LO electric coupling diagrams and the NLO magnetic moment coupling diagrams. In Fig. 4, the one pion interference term contributing to $d\sigma_2$ are plotted as the dashed curves at incident photon energies of 49 and 69 MeV. The angular distributions are dominated by the $(1+\cos^2\theta)$ factor that comes from the sum of the inner product squares of the incident and outgoing electric fields over the two different modes (electric fields parallel or perpendicular to the scattering plane). The small asymmetry comes from the finite size of the deuteron. The magnetic moment interference terms are plotted as the dotted curves. The $\cos\theta$ factor comes from the sum of the inner product of the incoming and outgoing electric fields times the inner product of the incoming and outgoing magnetic fields over the two different modes. The sum of the two terms that form the NLO contributions to $d\sigma_2/d\Omega$ are plotted as solid lines. The result is dominated by the pion interference terms. Higher order corrections could be as large as 30% of the contributions we show in this figure.

To indicate the relative size of $d\sigma_2$, we write the $J_z = 0$ and $J_z = \pm 1$ differential cross sections in terms of the unpolarized and tensor polarized differential cross sections, $d\sigma_0$ and $d\sigma_2$, as

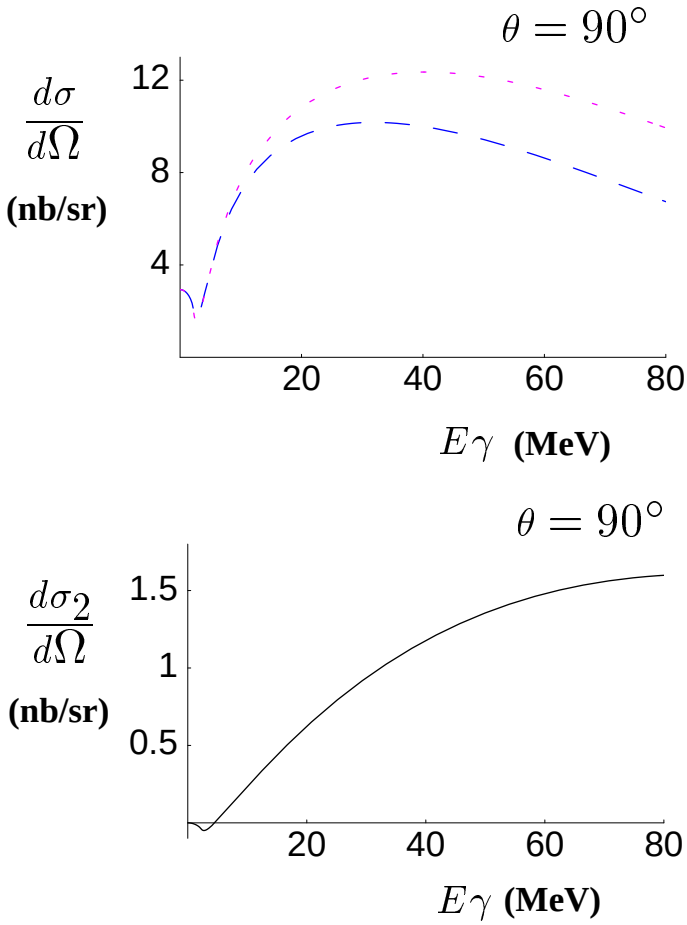

FIG. 6. *The differential cross section for polarized γ-deuteron Compton scattering at 90°. The dotted curve corresponds to the NLO deuteron $J_z = 0$ result. The dashed curves corresponds to the NLO deuteron $J_z = 1$ result. The solid curve corresponds to the tensor polarized result which is half of the difference between the dotted and dashed curves.*

$$\frac{d\sigma}{d\Omega}(J_z = 0) = \frac{d\sigma_0}{d\Omega} + \frac{4}{3}\frac{d\sigma_2}{d\Omega} \quad ,$$
$$\frac{d\sigma}{d\Omega}(J_z = \pm 1) = \frac{d\sigma_0}{d\Omega} - \frac{2}{3}\frac{d\sigma_2}{d\Omega} \quad . \tag{2.16}$$

The unpolarized differential cross section,

$$\frac{d\sigma_0}{d\Omega} = \frac{\alpha^2}{2M_N^2}\left[\left(|F_0|^2 + |G_0|^2\right) \ (1+\cos^2\theta) + 4Re\left[F_0 G_0^*\right]\cos\theta \right] \quad , \tag{2.17}$$

up to NLO can be found in [28]. Note that we have used $d\sigma(\ J_z = +1) = d\sigma(\ J_z = -1)$ in eq. (2.16) as photons are not circularly polarized. This is a consequence of parity conservation. In Fig. 5, we plot the $J_z = 0$ and $J_z = \pm 1$ differential cross sections as dotted and dashed curves respectively at photon energies of 49 and 69 MeV. The difference between each set of dotted and dashed curves gives $2d\sigma_2/d\Omega$ while the weighted sum gives $d\sigma_0/d\Omega$. At both energies, $d\sigma_2/d\Omega$ at backward angles can be extracted if the error bars in $J_z = 0$ and $J_z = \pm 1$ differential cross sections are $\sim 10\%$, as that of the unpolarized experiment [1]

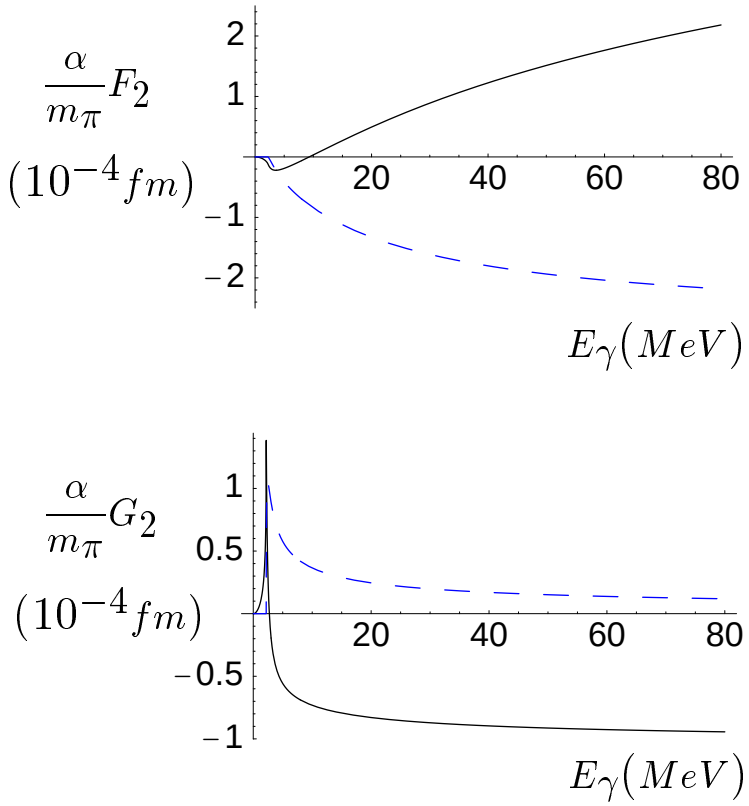

FIG. 7. *Form factors F_2 and G_2 calculated to the first non-vanishing order (NLO) shown as functions of photon energy. The solid lines are real parts and the dashed lines are imaginary parts.*

performed four years ago. With error bars of 4%, the forward angle part of $d\sigma_2/d\Omega$ would also be measurable. In these estimates, we have assumed that the higher order corrections to $d\sigma_2/d\Omega$ are 30%.

We can isolate the one pion interference term from $d\sigma_2^{NLO}$ by going to $\theta = 90^\circ$. As can easily be seen from eq. (2.15), at $\theta = 90^\circ$ the magnetic interference term vanishes. This provides a clean way to study the photon pion dynamics in the two nucleon sector. In Fig. 6, the NLO differential cross sections at $\theta = 90^\circ$ for deuteron polarizations $J_z = 0$ and $J_z = \pm 1$ are plotted as the dotted and dashed curves while $d\sigma_2/d\Omega$ is plotted as the solid curve. Again, with measurements of the $J_z = 0$ and ± 1 polarization made to within 7%, the pion interference term effects would be observable for photon energies between 40 and 80 MeV with the higher order effect estimated to be 30%. Note that the effective field theory expansion power counting is expected to break down at photon energy of about 100 MeV (recent works by Mehen and Stewart [26] suggest that in fact the breakdown scale may be much higher). But the neglected NLO terms which are suppressed by factors of $\mathbf{k^2}/m_\pi^2$ could contribute a 30% effect at 80 MeV. Thus the 80 MeV photon energy sets an upper bound for the calculations performed in this paper.

It is also interesting to compare our results with those from potential model calculations [32,33]. In Fig. 7, we show the fist non-vanishong order (NLO) results of F_2 and G_2 multiplied by a constant to compare with the form factors $P2(E1, E1)$ and $P2(M1, M1)$ calculated

and plotted in [32]. The agreement on G_2 is $\sim 10\%$ while the agreement on F_2 is $\sim$ 30-40%.

III. CONCLUSIONS

We have presented analytic expressions for the differential cross section of tensor polarized γ-deuteron Compton scattering in an effective field theory expansion. The first non-vanishing contributions are the interference terms between the leading electric coupling diagrams and the subleading single potential pion exchange diagrams, and between the leading electric coupling diagrams and the subleading magnetic moment coupling diagrams. At 90° photon scattering angle, only the pion term contributes at this order to the tensor polarized differential cross section. This provides a clean way to study the photon pion dynamics in the two nucleon sector. For photon energy between 40 and 80 MeV, the one pion interference term contributions would be measurable at 90° provided the uncertainty in the γ-deuteron Compton scattering experiments are $\lesssim 7\%$. At backward angles, the magnetic interference term adds to the pion term to give an effect which could be seen if the uncertainty in the measurements are $\lesssim 10\%$.

The author would like to thank Martin Savage, Roxanne Springer, Harald Griesshammer, Jerry Miller, Jon Karakowski ,and Daniel Phillips for helpful discussions and Hartmuth Arenhovel for correspondence. This work is supported in part by the U.S. Dept. of Energy under Grants No. DE-FG03-97ER41014.

REFERENCES

[1] M. A. Lucas, Ph. D. thesis, University of Illinois at Urbana-Champaign (1994).

[2] M.I. Levchuk and A.I. L'vov, *Few Body Systems Suppl.* **9**, 439 (1995).

[3] T. Wilbois, P. Wilhelm and H. Arenhovel, *Few Body Systems Suppl.* **9**, 263 (1995).

[4] J. Karakowski and G. Miller, `nucl-th/9901018`.

[5] S. Weinberg, *Phys. Lett.* B **251**, 288 (1990); *Nucl. Phys.* B **363**, 3 (1991); *Phys. Lett.* B **295**, 114 (1992).

[6] C. Ordonez and U. van Kolck, *Phys. Lett.* B **291**, 459 (1992); C. Ordonez, L. Ray and U. van Kolck, *Phys. Rev. Lett.* **72**, 1982 (1994) ; *Phys. Rev.* C **53**, 2086 (1996) ; U. van Kolck, *Phys. Rev.* C **49**, 2932 (1994).

[7] T.S. Park, D.P. Min and M. Rho, *Phys. Rev. Lett.* **74**, 4153 (1995) ; *Nucl. Phys.* A **596**, 515 (1996).

[8] D.B. Kaplan, M.J. Savage and M.B. Wise, *Nucl. Phys.* B **478**, 629 (1996).

[9] T. Cohen, J.L. Friar, G.A. Miller and U. van Kolck, *Phys. Rev.* C **53**, 2661 (1996).

[10] D. B. Kaplan, *Nucl. Phys.* B **494**, 471 (1997).

[11] T.D. Cohen, *Phys. Rev.* C **55**, 67 (1997). D.R. Phillips and T.D. Cohen, *Phys. Lett.* B **390**, 7 (1997). K.A. Scaldeferri, D.R.Phillips, C.W. Kao and T.D. Cohen, *Phys. Rev.* C **56**, 679 (1997). S.R.Beane, T.D. Cohen and D.R. Phillips, *Nucl. Phys.* A **632**, 445 (1998).

[12] J.L. Friar, Few Body Syst. **99**, 1 (1996).

[13] M.J. Savage, *Phys. Rev.* C **55**, 2185 (1997).

[14] M. Luke and A.V. Manohar, *Phys. Rev.* D **55**, 4129 (1997).

[15] G.P. Lepage, `nucl-th/9706029`, Lectures given at 9th Jorge Andre Swieca Summer School: Particles and Fields, Sao Paulo, Brazil,16-28 Feb 1997.

[16] S.K. Adhikari and A. Ghosh, J. Phys. **A30**, 6553 (1997).

[17] K.G. Richardson, M.C. Birse and J.A. McGovern, `hep-ph/9708435`; `hep-ph/9807302`.

[18] P.F. Bedaque and U. van Kolck, *Phys. Lett.* B **428**, 221 (1998); P.F. Bedaque, H.-W. Hammer and U. van Kolck, *Phys. Rev.* C **58**, R641 (1998); *Phys. Rev. Lett.* **82**, 463 (1999).

[19] U. van Kolck, Talk given at Workshop on Chiral Dynamics: Theory and Experiment (ChPT 97), Mainz, Germany, 1-5 Sep 1997.`hep-ph/9711222`

[20] T.S. Park, K. Kubodera, D.P. Min and M. Rho, *Phys. Rev.* C **58**, R637 (1998); *Nucl. Phys.* A **646**, 83 (1999).

[21] J. Gegelia, `nucl-th/9802038`; `nucl-th/9806028`.

[22] J.V. Steele and R.J. Furnstahl, *Nucl. Phys.* A **637**, 46 (1998); *Nucl. Phys.* A **645**, 439 (1999).

[23] D.B. Kaplan, M.J. Savage and M.B. Wise, *Phys. Lett.* B **424**, 390 (1998); *Nucl. Phys.* B **534**, 329 (1998);

[24] D.B. Kaplan, M.J. Savage, and M.B. Wise, *Phys. Rev.* C **59**, 617 (1999).

[25] T. Cohen and J.M. Hansen, *Phys. Lett.* B **440**, 233 (1998); *Phys. Rev.* C **59**, 13 (1999).

[26] T. Mehen and I.W. Stewart, *Phys. Lett.* B **445**, 378 (1999); `nucl-th/9809095`.

[27] E. Epelbaoum, W. Glockle, A. Kruger and Ulf-G. Meissner, *Nucl. Phys.* A **645**, 413 (1999).

[28] J. W. Chen, H. W. Grießhammer, M.J. Savage, and R. P.Springer, *Nucl. Phys.* A **644**, 221 (1998).

[29] J. W. Chen, H. W. Grießhammer, M.J. Savage, and R. P.Springer, *Nucl. Phys.* A **644**, 245 (1998).
[30] M.J. Savage and R.P. Springer, *Nucl. Phys.* A **644**, 235 (1998). D.B. Kaplan, M.J. Savage, R.P. Springer and M.B. Wise, *Phys. Lett.* B **449**, 1 (1999).
[31] K. Coulter *et al.*, *Phys. Rev. Lett.* **68**, 174 (1992).
[32] M. Weyrauch and H. Arenhovel, *Nucl. Phys.* A **408**, 425 (1983).
[33] M. Weyrauch, *Phys. Rev.* C **41**, 880 (1990).